Inhibitively Coupled Chemical Oscillators as a Substrate for Logic Gates and Larger Circuits

Jacob M. Gold

May 7, 2015

Abstract

We investigate the Belousov-Zhabotinsky (BZ) reaction in an attempt to establish a basis for computation with inhibitively coupled chemical oscillators. The system consists of BZ droplets suspended in oil. Interdrop coupling is limited to the non-polar inhibitory species Br_2. We consider a linear arrangement of droplets to be a NOR gate, where the center droplet is the output and the other two are inputs. Oxidation spikes in the inputs, which we define to be TRUE, cause a delay in the next spike of the output, which we read to be FALSE. Conversely, when the inputs do not spike (FALSE) there is no delay in the output (TRUE). We are able to reliably produce NOR gates with this behavior in microfluidic experiment. We also discuss potential future methods for connecting multiple gates to form larger circuits.

Contents

1 Introduction **2**
1.1 Chemical Computation 2
1.2 The Belousov-Zhabotinsky Reaction 3

2 Experiments **13**
2.1 NOR Gate 13
2.2 Experimental System 17
2.3 Results 19

3 Discussion **28**
3.1 Conclusion 28
3.2 Future Work 29

4 Bibliography **34**

A Supplemental Information **38**
A.1 FKN Mechanism 39
A.2 Simulation Parameters 40

Chapter 1

Introduction

We provide background on chemical computation, particularly past work which utilizes the Belousov-Zhabotinsky (BZ) reaction. We then describe the BZ reaction in greater detail, and how to model the interactions between BZ microdroplets.

1.1 Chemical Computation

Computers are ubiquitous in everyday life. While anything that performs arithmetic or logical operations can be considered to be computer, the word is most often associated with universal computers. A universal computer can be programmed to carry out any number of arithmetic and logical operations, as described by a Turing machine [22]. While a theoretical Turing machine has unlimited memory on its infinite tape, the average desktop composed of integrated circuits is as close as possible to a universal computer since it has more than enough memory for practical purposes.

In recent years there has been interest in what systems other than electronic circuits can be used to perform computation. For example, it has been shown that DNA [14, 16], microfluidic systems [17], and slime molds [1, 21] are all capable of supporting computation. Demonstrating that such a system can support computation generally involves showing that it can represent different states of a Turing machine, often through the use of binary logic gates.

A considerable amount of work has been done demonstrating various ways computation can be implemented in reaction-diffusion systems [2]. The BZ reaction is particularly well-suited for this task due to the ability to use excitatory waves to propagate a signal through a circuit. Often the interactions of multiple wavefronts are used to compute the output of binary logic gates dependent on the geometry of the medium through which the waves travel [10, 18], but it is possible to define a binary logic in an open system as well [4]. Computation with waves generally relies on excitatory coupling, but our group has also investigated the feasibility of waves in domains which are inhibitively coupled [9].

1.2 The Belousov-Zhabotinsky Reaction

The BZ reaction is an oscillating chemical reaction in which malonic acid is periodically oxidized by acidic bromate. As one of the first oscillating chemical reactions discovered [3] it has become the prototypical reaction

with periodic behavior. The BZ reaction has been used to study nonlinear dynamics [8] and morphogenesis [20] as well as computation.

In our experiments the acidic conditions are maintained through the use of sulfuric acid. We use the indicator ferroin which changes from red to blue when it is oxidized to ferriin. We also introduce the photosensitive catalyst ruthenium-tris(2,2-bipyridyl) (Rubpy) [20]. The BZ reaction can be described by the Field-Koros-Noyes (FKN) mechanism [13, 15] (see appendix A.1 for full reaction). The corresponding differential equations are:

$$\frac{\mathrm{d}x}{\mathrm{d}t} = -k_1xy + k_2y - 2k_3x^2 - k_4x + k_rw^2 + k_{red}wc \tag{1.1}$$

$$\frac{\mathrm{d}y}{\mathrm{d}t} = -k_1xy - k_2y - k_5yp + k_6u + k_7u + k_9z + k(I)\frac{bc}{b_c + b} \tag{1.2}$$

$$\frac{\mathrm{d}z}{\mathrm{d}t} = k_{red}wc - k_9z - k_{10}z + k(I)\frac{bc}{b_c + b} \tag{1.3}$$

$$\frac{\mathrm{d}p}{\mathrm{d}t} = 2k_1xy + k_2y + k_3x^2 - k_5yp + k_6u - k_8p \tag{1.4}$$

$$\frac{\mathrm{d}u}{\mathrm{d}t} = k_5yp - k_6u - k_7u \tag{1.5}$$

$$\frac{\mathrm{d}w}{\mathrm{d}t} = 2k_4x - 2k_rw^2 - k_{red}wc \tag{1.6}$$

$$\frac{\mathrm{d}c}{\mathrm{d}t} = -k_{red}wc + k_9z + k_{10}z - k(I)\frac{bc}{b_c + b} \tag{1.7}$$

where the function $K(I)$ relates the activity of Rubpy to the intensity of light on the reactor [12].

There exists a stable, steady-state solution to these equations which results in the periodic oxidation of ferroin that occurs in experiment. Since the solution is periodic the trajectory of the solution in the space of chemical

concentrations forms a limit cycle [11]. When the system is known to be in the steady state, one can describe the entire state of the system with a single variable, the phase, which describes at what point in the limit cycle the system is currently at. The phase is often defined from 0 to 2π, but can also be defined from 0 to 1, as we will do here for ease of interpretation. Thus, the equation for a single uncoupled phase oscillator is the following:

$$\frac{\mathrm{d}\theta}{\mathrm{d}t} = \omega \tag{1.8}$$

In our experiments we produce a surfactant-stabilized [7] emulsion of aqueous BZ microdroplets suspended in oil [19]. Neighboring droplets are coupled purely through diffusion, and the surfactant limits diffusion to primarily the non-polar inhibitory species Br_2. The coupling strength between two droplets is a function of their size, geometry, the distance between them, the diffusion rate, and the partition coefficient of Br_2 in oil and water [20]. We use the Vanag-Epstein (VE) model [23] of the BZ reaction, which is simplified based on certain concentrations remaining constant or in quasiequilibrium

with other species:

$$\frac{\mathrm{d}x}{\mathrm{d}t} = -k_1xy + k_2y - 2k_3x^2 + k_4x\frac{(c_0 - z)}{c_0 - z + c_{min}} \tag{1.9}$$

$$\frac{\mathrm{d}y}{\mathrm{d}t} = -3k_1xy - 2k_2y - k_3x^2 + k_7u + k_9z + k(I)\frac{c_0 - z}{\frac{b_c}{b} + 1} \tag{1.10}$$

$$\frac{\mathrm{d}z}{\mathrm{d}t} = 2k_4x\frac{(c_0 - z)}{c_0 - z + c_{min}} - k_9z - k_{10} + k(I)\frac{c_0 - z}{\frac{b_c}{b} + 1} \tag{1.11}$$

$$\frac{\mathrm{d}u}{\mathrm{d}t} = 2k_1xy + k_2y + k_3x^2 - k_7u \tag{1.12}$$

There are simpler models that display some of the same behavior as the VE model but do not capture the same inhibitory coupling.

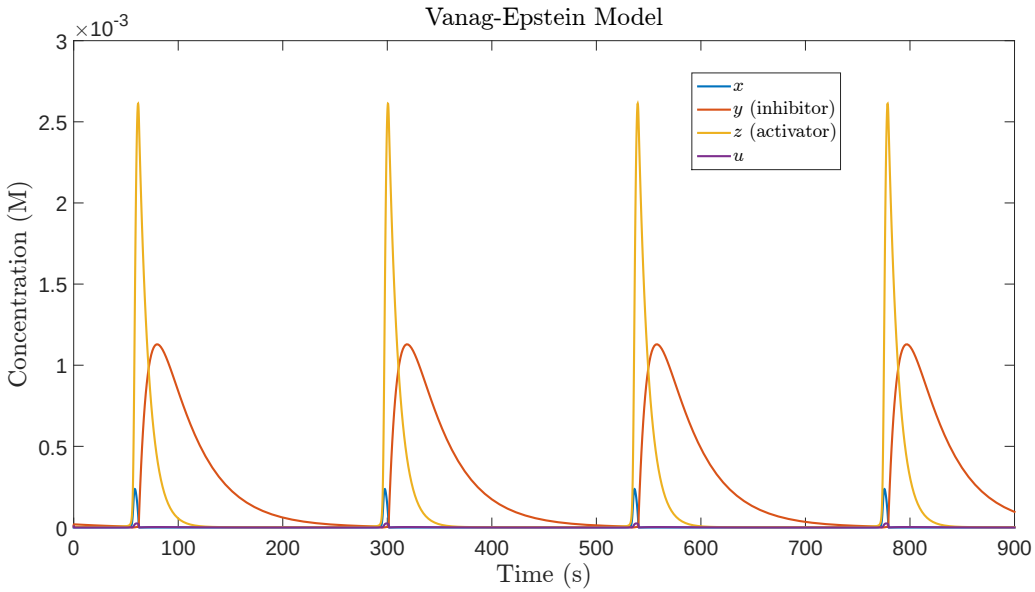

Figure 1.1: A plot of the numerical solution to the VE model for approximately four periods with zero light intensity. Notice the periodic spikes of z, the activator, followed by the production and decay of y, the inhibitor.

When using the Vanag-Epstein model to describe a system of coupled

droplets, we treat each droplet as a well-mixed reactor with four chemical concentrations, then add a coupling term equal to the coupling strength K times the difference in y between two given drops.

$$\frac{\partial y_i}{\partial t} = K(y_j - y_i) \tag{1.13}$$

Since weakly coupled drops oscillate near the limit cycle, we can still describe the state of each one with a single phase variable. We define phase 0 to be when the concentration of oxidized indicator is at a maximum. Just after this oxidation spike, the concentration of inhibitor in a droplet will also reach its peak. Some of this inhibitor will diffuse into neighboring droplets, pushing them back along their limit cycles. This results in a delay of the next oxidation spike of those neighboring drops, or negative phase shift. The result of this inhibitory coupling is that in the steady state a network of droplets will have each drop spiking as far away in time from the spikes of other drops as possible. In the case of two coupled drops their spikes will be antiphase [5].

When using a phase variable to describe the state of each droplet the interactions between droplets must also be defined as a function of their phases. In the most general form, the differential equation for the ith reactor becomes

$$\frac{\mathrm{d}\theta_i}{\mathrm{d}t} = \omega + \sum_j H_i(\theta_i, \theta_j) \tag{1.14}$$

where j is summed over each reactor the ith is coupled to. The function H

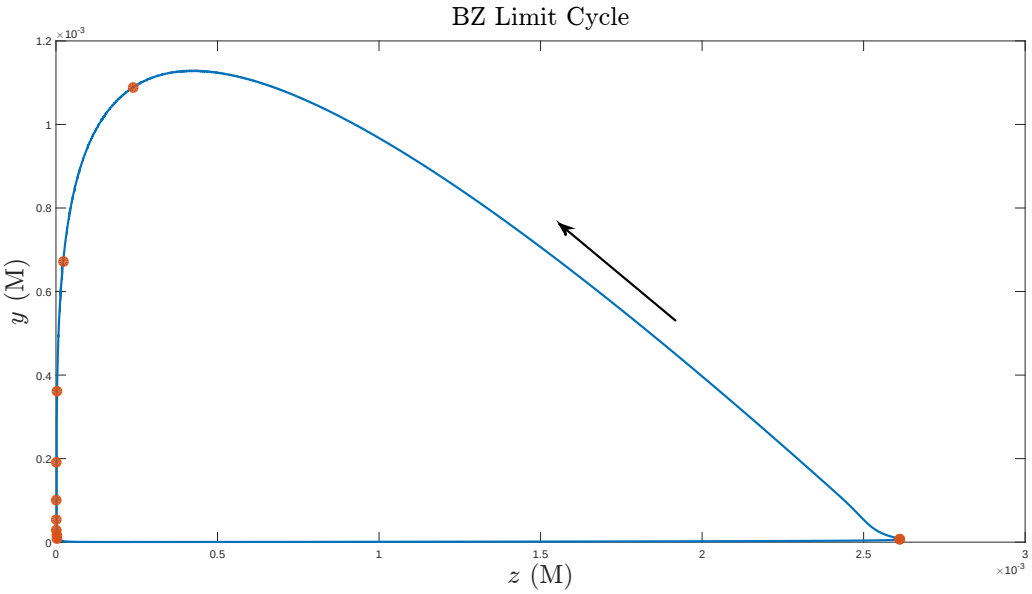

Figure 1.2: A phase plot of the limit cycle, plotting the excitatory species z against the inhibitory species y. Ten points equidistant in time have been overlayed to demonstrate that the majority of the period is spend in the region where z concentration is low.

which describes the interactions between two oscillators is known as the coupling function. To find this function exactly one must consider the isochrons of the limit cycle the oscillators sit on. An isochron is made of points off the limit cycle that after a length of time equal to some multiple of the period of an oscillator will sit at a point on the limit cycle with phase p; these points can be considered to also have phase p. When a chemical perturbation is applied to an oscillator at some phase, it will shift the oscillator from the limit cycle in the chemical space to an isochron with some other phase. Measuring what this shift is for every phase along the limit cycle allows for the creation of a phase response curve (PRC). In the case of weak coupling one can as-

sume that the phase shift is linear in the size of the chemical perturbation, so one can find the coupling function of two drops by multiplying the PRC of the drop being perturbed by the amount of inhibitor diffusing from the neighboring drop, which can be determined from the phases of both drops. Therefore,

$$\frac{\mathrm{d}\theta_i}{\mathrm{d}t} = \omega + \sum_j \varphi(\theta_i)(\chi(\theta_j) - \chi(\theta_i)) \tag{1.15}$$

where $\varphi(\theta)$ is the response of a drop and $\chi(\theta)$ is the concentration of inhibitor in a drop at phase θ.

The isochrons of the limit cycle for the BZ reaction can be found numerically by integrating the negative of the differential equations with initial conditions near the limit cycle with a known period, which can be then be used to find the PRC for a single droplet. In practice there are more efficient ways to find the PRC, which we do through simulations using the Vanag-Epstein model. One way is to start by initializing two coupled BZ drops at two particular phases and integrating the equations for a length of time much less than the period of one drop. The drops are then uncoupled and the trajectory of the first drop is found until it reaches an oxidation spike. The length of time until this spike occurs is compared to how long it would take an uncoupled drop starting from the same initial phase to spike. The difference divided by the period is equal to the phase shift.

$$H_i(\theta_i, \theta_j) = \Delta\theta_i = \frac{-t_{i,spike,coupled} + t_{spike,uncoupled}}{T} \tag{1.16}$$

This process is repeated with the length of time the two drops are coupled for progressively shortened. A regression is then used to find the phase shift in the limit as the coupled time goes to zero as a function of the phases of each drop (figure 1.3).

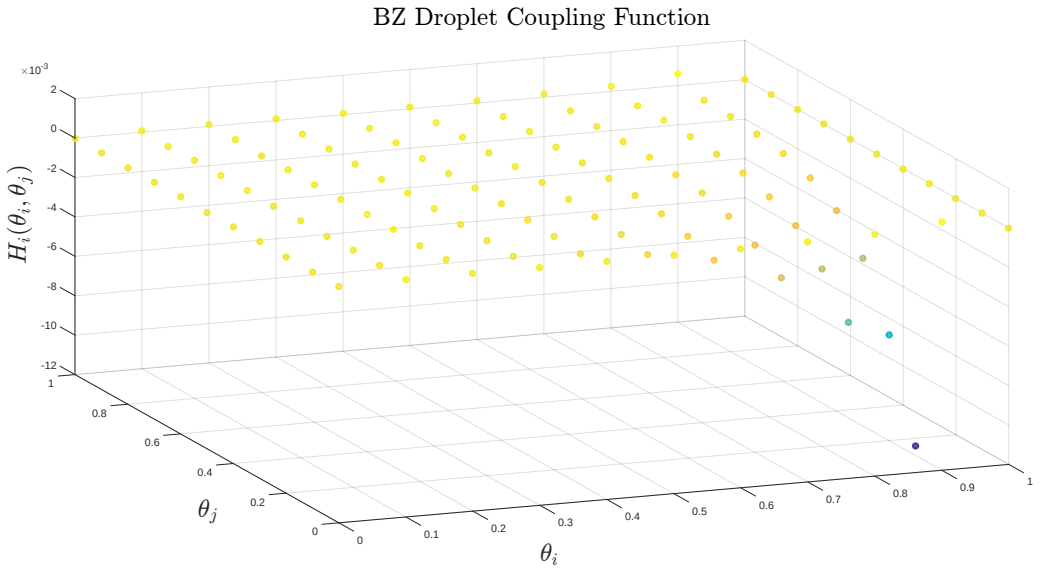

Figure 1.3: A scatter plot of the coupling function H measured by taking $\lim_{t\to 0} \Delta\theta$ where t is the amount of time two drops using the VE model are coupled. The value of H is calculated with $T = 240$s. H is negative everywhere since coupling between drops is only inhibitory. The phase θ_i when the drop is most susceptible to perturbation corresponds to the state when the concentration of inhibitor in the drop is lowest. The phase θ_j when the neighbor perturbs the drop the most corresponds to just after an oxidation spike, when the neighbor will produce the most inhibitor.

Another PRC that we calculate which has more applications to our later experiments is the response when the perturbed droplet is coupled for most of one period to a drop which is initialized at an oxidation spike (figure 1.4, figure 1.5). We use 4/5 of a period, as the previous PRC makes it clear that

the perturbing drop has little effect during the last 1/5 of its period. We do not use an entire period as the amount of inhibitor produced starts to increase before the peak of indicator is reached, as in our experiments we control our perturbing drops such that they only spike once.

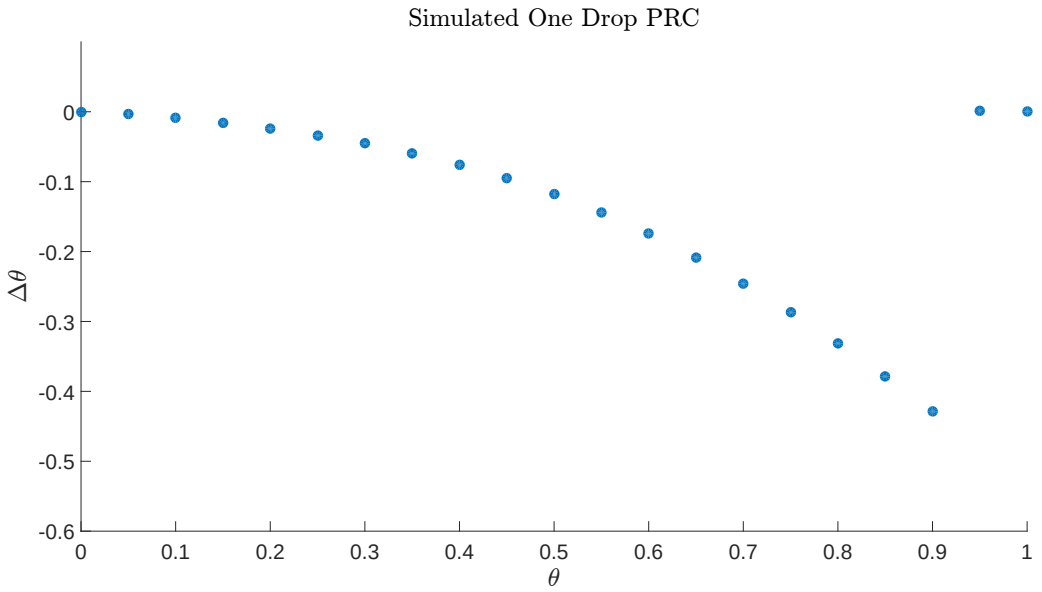

Figure 1.4: A scatter plot of the PRC of a BZ drop simulated with the VE model. The drop being perturbed is coupled to a drop initialized to an oxidation spike for 4/5 of a period. Similar to figure 1.3, the PRC is negative everywhere, and the drop is most susceptible to perturbation in the state when inhibitor concentration is at a minimum.

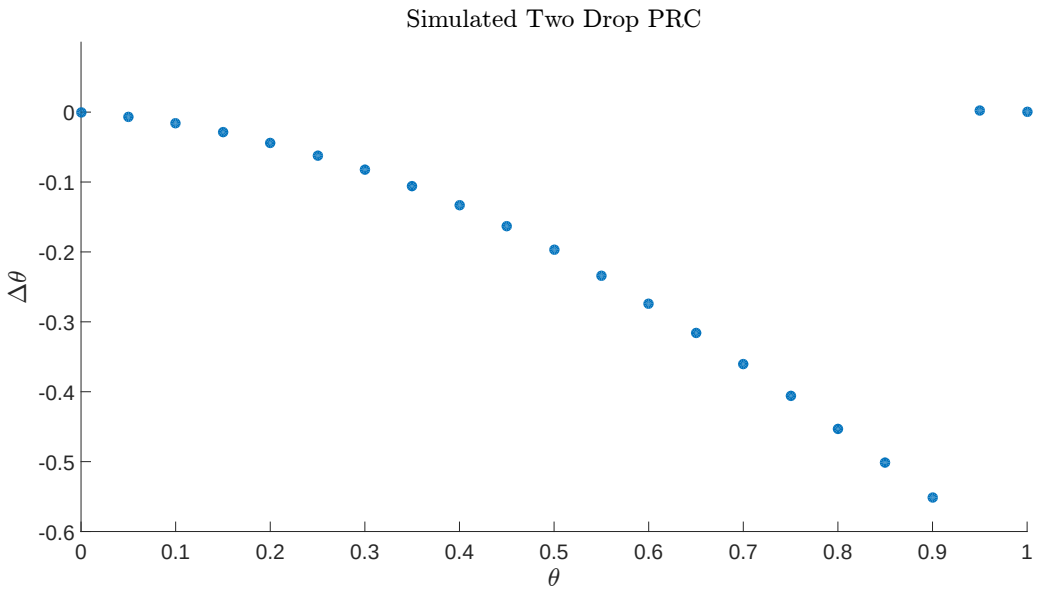

Figure 1.5: A scatter plot of the PRC of a BZ drop simulated with the VE model. The drop being perturbed is coupled to two drops initialized to an oxidation spike for 4/5 of a period. Note that the response for any given phase is not twice the response in figure 1.4; this is due to the nonlinearity of the BZ reaction.

Chapter 2

Experiments

We define what we consider to be a NOR gate in our experimental system. We describe the system and equipment we use to investigate the NOR gate. We present the results of experiments which characterize the BZ reaction, then the results of experiments informed by those characterizations where we test the functionality of the NOR gate.

2.1 NOR Gate

Since our system consists of well-mixed BZ oscillators, we are able to formulate a description of computation based on discrete chemical pulses instead of waves. Using such a system to perform computation is based on the idea that neurons, often modeled as coupled oscillators [6], produce computation in the brain. We choose to investigate the feasibility of constructing a NOR

gate, since in the scenario where we are able to connect multiple gate in series and parallel we will be able to synthesize any other circuit.

A NOR gate is a two-input logic gate which outputs TRUE when both inputs are FALSE, and outputs FALSE when one or both of the inputs are TRUE. To construct a NOR gate out of BZ droplets we need to leverage their dynamics in such a way that they satisfy this definition. The simplest choice for a TRUE input signal is an oxidation spike in a drop indicated as the input to our gate, so a FALSE signal is a lack of oxidation spike. For our gate to have the proper behavior we must define the output in such a way that when one or both of our input droplets have an oxidation spike, the behavior of our output is distinguishable from the case when neither input spikes, but the difference between one and two spikes is indistinguishable.

Since any oxidation spike in one droplet results in the diffusion of inhibitor to its neighbors, we can produce the desired behavior for our NOR gate by designating the droplet between two input droplets to be our output droplet. If either of the inputs spike they will inhibit the oscillation of the output, causing its spike to arrive later than would otherwise be expected. Since the output droplet will always eventually spike, we differentiate this from the case when neither input peaks through the use of a reading frame. We measure when the output is expected to spike based on its natural period, and we also measure the delay we expect from one or two spikes. We choose a temporal window which ends after the output is expected to spike naturally but before it would spike if perturbed. By defining a spike before the window ends to

be TRUE and after it ends to be FALSE, we can produce the behavior of a NOR gate.

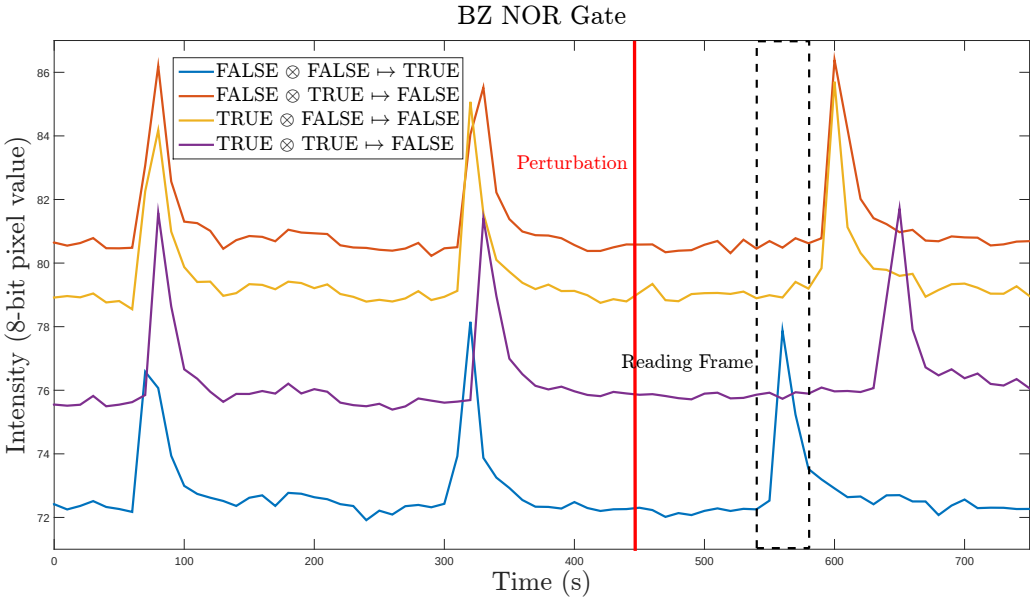

Figure 2.1: Intensity traces from experiment showing the behavior of a NOR gate for the four possible input cases. Between the first two oxidation spikes in each case the period is measured to determine when to stop suppressing the inputs, and the perturbation occurs between the second and third spikes, resulting in a delay in three of the four cases. These cases can be differentiated through the use of a reading frame. If the output spikes in the reading frame, it is interpreted as TRUE; if not, it is FALSE.

There are several factors we must measure to characterize our gate and verify that it functions reliably. First, the delay of the peak of the output following a perturbation from an input must be significant enough that our reading frame correctly differentiates between TRUE and FALSE outputs. A larger delay means this can be accomplished more consistently. To maximize the delay resulting from a perturbation, we consult the PRC. Having

our inputs peak when they will produce the most negative phase shift, corresponding to the largest delay, will result in the optimal gate behavior. We measure the PRCs for the case of perturbations from one or both inputs.

We suppress our input drops with light while they are not being used. If we want to send a FALSE input, the drop simply remains suppressed, so it will not perturb its neighbors. If we want to send a TRUE input, we cease illuminating it until it peaks once, then resume illumination. Since we aim to have our inputs peak at a particular phase of the output droplet, we must measure the amount of time we expect to wait for them to peak once we remove light from them; finding this input delay is the second step to characterizing our gate.

We also must consider measure the magnitude of the variations in these characteristics. This includes statistical variation, such as the standard deviation of the phase shift resulting from a perturbation, but also includes variations intrinsic to our system. As the BZ reaction progresses, catalyst and malonic acid are consumed, which may change the period of oscillation and the coupling strength between drops. While our observations show that these variations do have significant effects on the performance of our NOR gates, it is difficult to predict some behaviors such as period change over time as we see different trends from experiment to experiment.

2.2 Experimental System

We conduct our experiments with 2D arrays of BZ droplets. The droplets are fabricated with a PDMS microfluidic chip where two streams of reactants flow together to form droplets separated by oil. The first stream contains 400mM malonic acid, 80mM sulfuric acid, and 2.5 mM sodium bromide, and the second stream contains 300mM sodium bromate, 3mM ferroin, and 1.2mM Rubpy. The reactants are separated such that no reaction will take place until the two streams are mixed, and the sodium bromide included provides a short additional delay until oscillations begin. The droplets have a period of oscillation ranging from 240 to 300 seconds and a reaction lifetime of approximately 100 oscillations. We load our droplets into a rectangular capillary with inner dimensions of 0.1mm x 2.0mm. The droplets are approximately 150um in diameter, and will hexagonally pack when loaded.

We perform our experiments with the use of a programmable illumination microscope (PIM). We light our sample with green (λ = 510 nm) Kohler illumination since it is absorbed by ferroin but transmits through feriin, and does not interact with rubpy. We are also able to project blue light (λ = 450 nm) onto specific droplets to suppress their oscillations. We record images of the sample every ten seconds.

When running an experiment we use image processing to identify each droplet in our sample and determine whether light should be projected on it for three seconds until the next image is recorded. If droplets move between

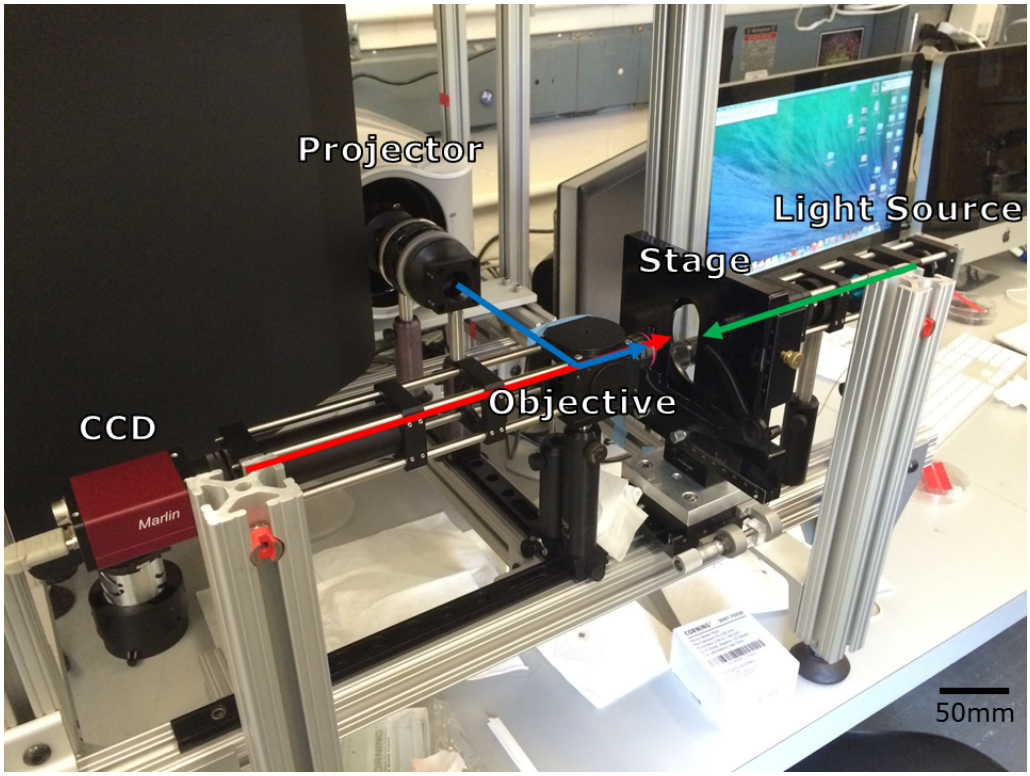

Figure 2.2: The PIM we use to conduct experiments. The stage lies in the focal plane of a light source which illuminates our sample, a CCD which we use to record images of our sample, and a commercial overhead projector which we use to optically suppress droplets in our sample.

when two images are recorded it is still possible to identify which drops should have light projected on them as long as they move a distance less than that of a drop radius. We are able to create constant chemical boundary conditions around any subset of the drops by selectively illuminating each drop bordering that subset.

2.3 Results

Our first experiments measure the PRC of a BZ droplet when perturbed by the oxidation spike of one or two neighbors (figure 2.4 and figure 2.5, respectively). To accomplish this we begin by optically isolating the droplets for which we are measuring the PRC. We wait until enough images are recorded of the droplets that their periods can be accurately measured. The period is calculated based on the amount of time between the most recent spike and the one preceding it. Each frame a phase is calculated for every droplet based on the period and the length of time since the previous spike. Once a droplet is at the phase we want to measure the response for we stop illuminating one or two of its neighbors. The light remains off of the neighbors until they spike, at which point we resume illumination. We calculate the response to this perturbation by comparing the amount of time between the next spike and the previous to the period measured before that, using equation 1.16. We repeat this process for a range of phases to map out the entire PRC, waiting several periods in between measurements to make sure our system returns to the limit cycle. While there is a delay between the removal of light from neighboring drops and their spikes we expect that the phases at which they actually spike will still be fairly evenly distributed. In our calculations for the PRC we use the phase at which the neighbors spike, not the phase we stopped suppressing them.

Once we have measured the PRCs for one and two spiking neighbors we

are able to decide on what phase we want to aim to perturb our output at in the NOR gate. Since we are trying to distinguish as much as possible the perturbed output from the unperturbed output we choose to have our inputs spike at the phase which results in the response of greatest magnitude, near $\theta = 0.85$. To be able to have our inputs function consistently we must measure the delay between when we stop suppressing them and when they spike so we can stop illuminating them that long before the output reaches the phase we want to perturb it at. We also examine the variation in this delay, since if it is too inconsistent we may end up attempting to perturb the output just after it has spiked as opposed to just before, so it will not be delayed at all. We find that the input delay tends to be slightly above half a period, plus or minus one tenth of a period.

With our characterization complete we can finally construct NOR gates in experiment. As with the PRC measurements we isolate our outputs be illuminating each neighboring drop. We designate two drops on opposite sides of the output to be the inputs; we stop suppressing them when we want to send a TRUE input, and continuously illuminate them otherwise. In cases where we do send a TRUE input, we stop suppressing our droplets such they spike at $\theta = 0.85$. We measure the phase shift for each input case (figure 2.6). As we are able to fit eight NOR gates into our field of view while ensuring two suppressed drops between them, we initially test each possible input case twice. We order the input cases FALSE $\otimes$ FALSE, FALSE $\otimes$ TRUE, TRUE $\otimes$ FALSE, and TRUE $\otimes$ TRUE, with the second

case referring to a TRUE signal at the input closer to the top of our sample, and the third case referring to a TRUE signal at the input closer to the bottom of our sample. After the first measurement is made with each gate, we wait several periods then use the same set of droplets to make another measurement. With the first set of input cases we shift the measurement made with a gate to the next one in our ordering, and with the second set we shift it to the previous. This ensures that any time-dependent effects on our NOR gate will be averaged out over the nth measurement made with each gate, but any geometry-dependent effects (e.g. a difference between the top and bottom inputs) will persist. We find that we are able to reliably produce NOR gates for the first two measurements made with each set of droplets, but as the experiment goes on chemical consumption increases the noise in both the phase that the inputs spike at and the resulting phase shift (figure 2.7, figure 2.8).

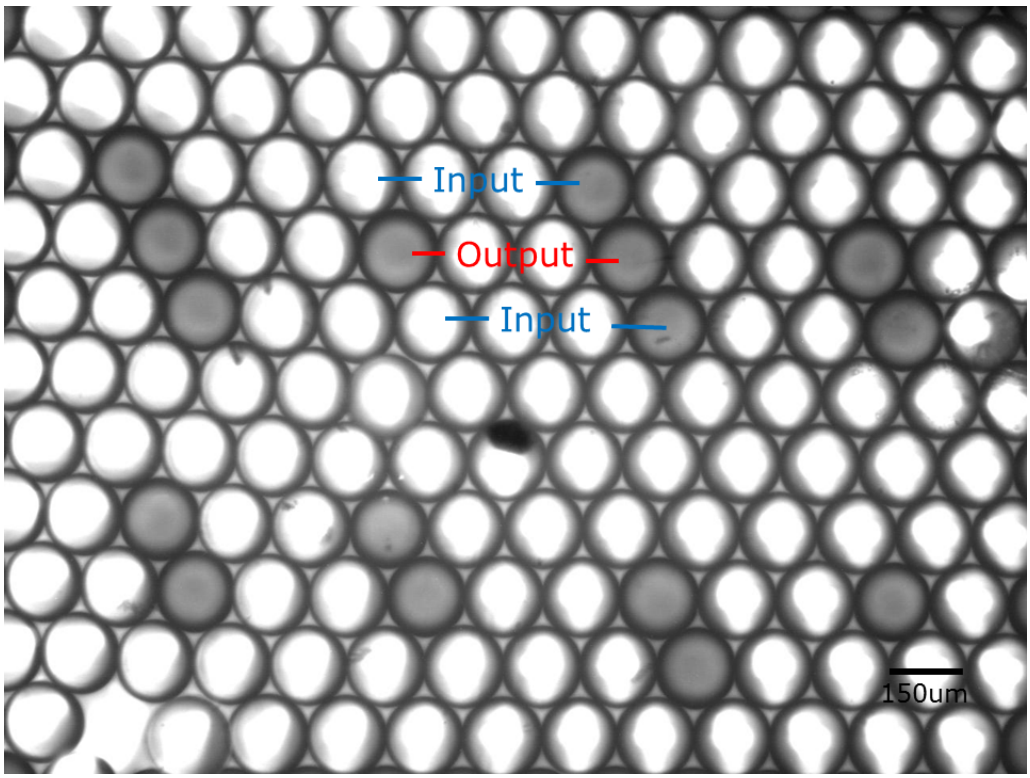

Figure 2.3: A frame recorded from an experiment of eight NOR gates, two in each possible input case. Note that each drop surrounding our gates in addition to each input not currently being used is illuminated as to suppress its oscillations. Of the two gates which are labeled, the one on the left has both inputs suppressed, so it is the FALSE $\otimes$ FALSE case, while the one on the right has both inputs about to spike, so it is the TRUE $\otimes$ TRUE case.

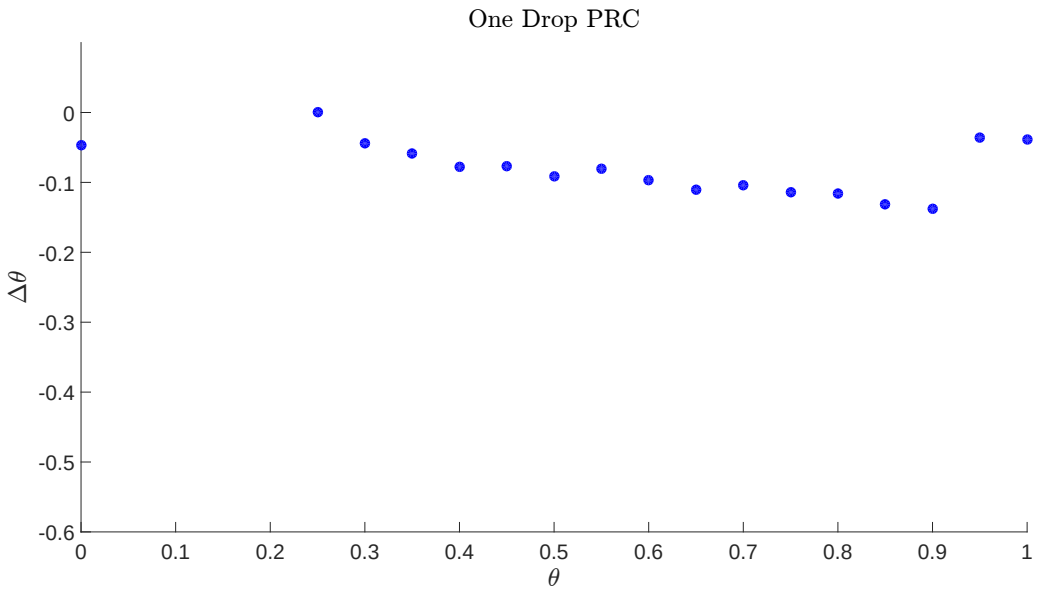

Figure 2.4: A scatter plot of the experimentally measured PRC of a BZ droplet. The perturbation we consider is diffusion from a neighbor which we stop suppressing until it spikes once. The phase of the perturbation is the phase of the drop we are measuring at which its neighbor spikes. The values have been binned ($n = 21$) and averaged, with some bins just after $\theta = 0$ having no data because in that region the spike of the neighboring drop will be delayed by the spike of the drop we are measuring.

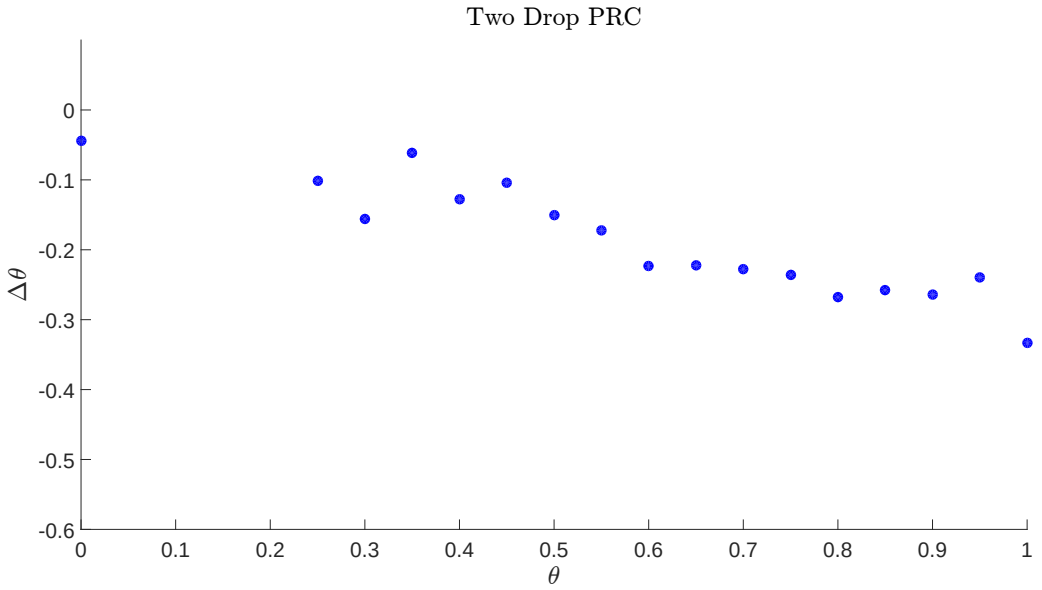

Figure 2.5: Another scatter plot of the experimentally measured PRC of a BZ droplet. The data is collected and presented in the same way as figure 2.4, except in this case the droplet is perturbed by the spikes of two neighbors simultaneously. The result is roughly twice the phase shift as the one drop PRC. Comparing our experimental results to our simulations (figure 1.4, figure 1.5) reveals that this behavior is not necessarily expected. Since the magnitude of the phase shifts also differ between simulation and experiment, it is reasonable to believe that the nonlinearity of the PRC is related to the coupling strength.

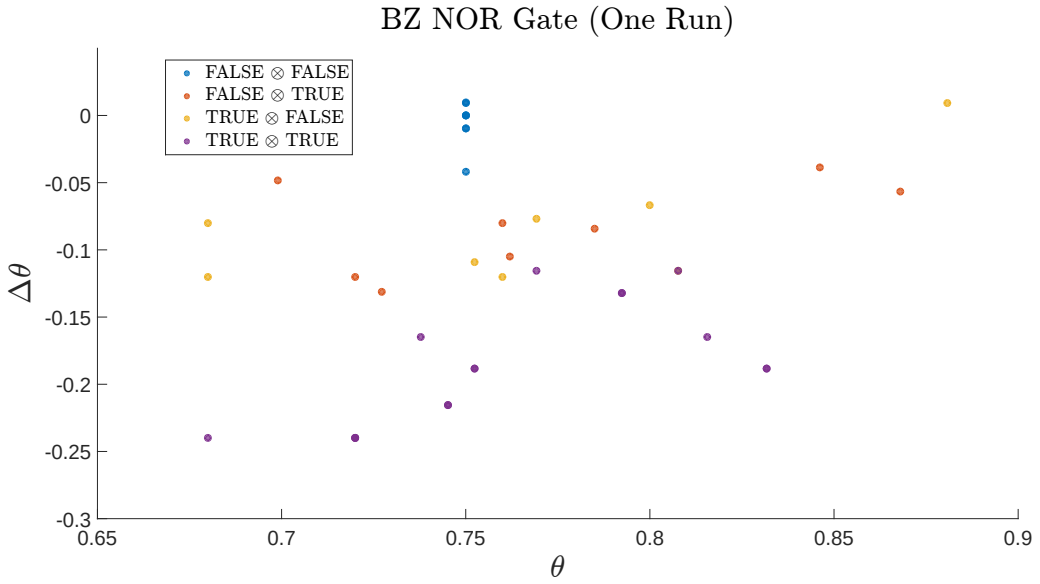

Figure 2.6: A scatter plot of data collected from a single experiment with an array of 8 NOR gates. Note that in general inputs with at least one TRUE signal cause a delay greater than that of the FALSE $\otimes$ FALSE case. While both inputs in the FALSE $\otimes$ FALSE case remain suppressed, we plot them at $\theta = 0.75$ for comparison. One would not expect a delay from this case, but the variation in measured period due to our limited temporal resolution can cause the appearance of a small phase shift. This is not problematic as other input cases still produce shifts large enough that the two cases can be differentiated.

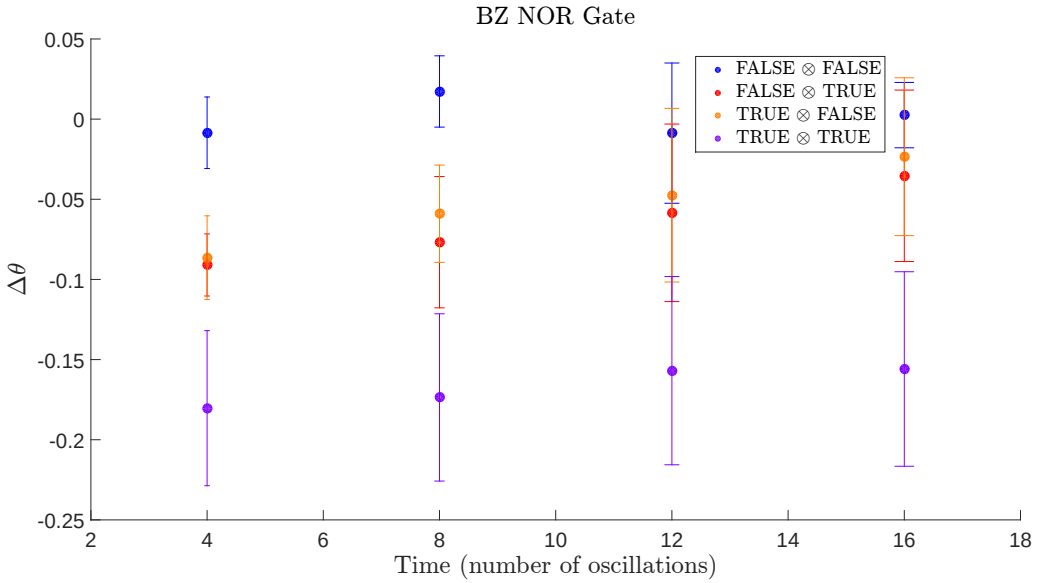

Figure 2.7: Plot of the mean phase shift for each input case averaged over 5 experiments, where each experiment consists of 8 NOR gates. The horizontal axis indicates how long our droplets have been oscillating when we measure a phase shift. Note that the variance when the drops have oscillated for and eight times is small enough that the FALSE ⊗ FALSE input case is significantly different from each other possible input. This means that one can choose the end of their reading window in such a way that it will correctly differentiate between TRUE and FALSE outputs. As chemicals are consumed our system becomes noisier and the difficulty of differentiating the input cases increases.

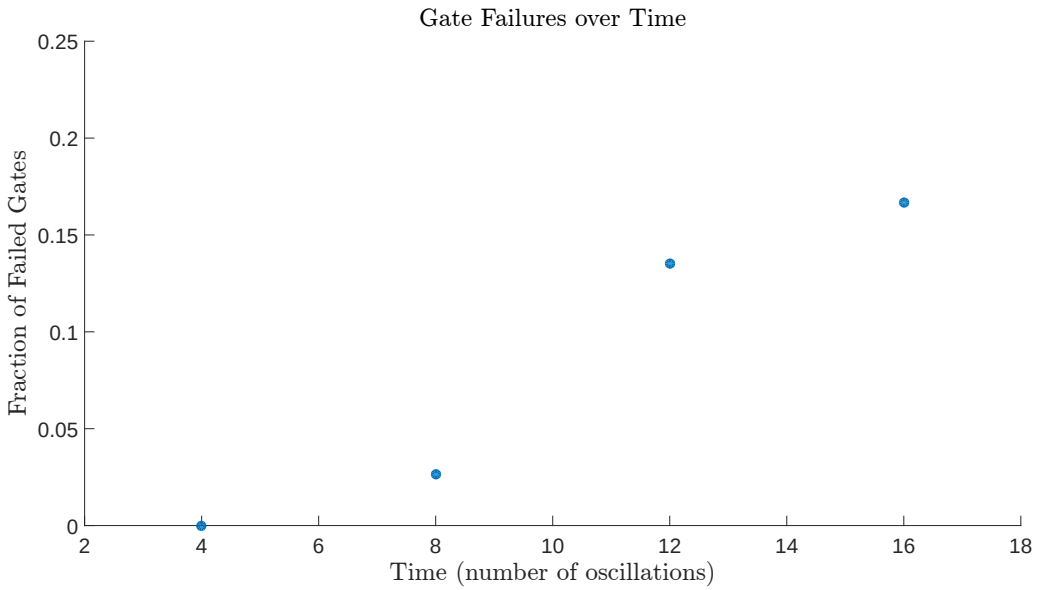

Figure 2.8: Plot of the fraction of NOR gates which fail as a function of how many times our drops have oscillated. A gate is considered to fail if an input which should produce a FALSE output produces less of a phase shift than the mean phase shift of TRUE outputs measured at the same time in the same experiment. For an experiment with 8 NOR gates there are 6 outputs which could potentially fail. After four oscillations our inputs have consumed so much photosensitive catalyst that they no longer oscillate.

Chapter 3

Discussion

We analyze what we were able to achieve in our experiments and how our method of computation compares to prior research. We also present future directions for our work, chiefly how one might connect multiple NOR gates to create larger circuits and achieve universal computation.

3.1 Conclusion

We have demonstrated that we are able to reliably produce NOR gates with BZ droplets. Most computation that has been done previously using reaction-diffusion systems relies on excitatory coupling, but we have shown that there is merit to systems with inhibitory coupling as well. Our system can be easily adapted to other experiments since the network of droplets can be reconfigured by changing which ones are suppressed, including in the mid-

dle of an experiment if desired. Investigations into engineering bio-inspired solutions to computational problems could lead to the creation of systems which process information in a way more similar to humans than electronic circuits.

3.2 Future Work

While we are now able to reliably construct NOR gates from BZ droplets, there is still room for improvement at the level of a single gate. The larger the phase shift that results from a TRUE input, the more we can differentiate between TRUE and FALSE outputs; a phase shift of 0.5 would be ideal. We can achieve greater phase shifts than our current experiments by increasing the coupling strength between drops. One simple way to do this is to decrease the size of the drops we use. The droplets we use are 150um in diameter, but we are able to produce droplets down to 50um fairly consistently.

Another way to improve our current system is to move from a closed to an open system, where we flow in additional reagents to counteract the decrease in reliability of our NOR gates over time. This could be achieved by switching from droplets in a glass capillary to droplets in a PDMS chip. The size of the pores in PDMS are small enough that the excitatory species, $HBrO_2$, cannot diffuse through it, but the inhibitory species, Br_2, can. We would design our chip to have walls separating compartments containing BZ solution so they are inhibitively coupled, then have channels connected to

these compartments where we flow in new chemicals.

A more interesting problem to consider is how to connect multiple BZ NOR gates to create larger circuits. The most naive way to do this is to see what happens when the output of one NOR gate in used as the input to another gate. We will consider all droplets that are not being controlled optically to start out in the steady state, meaning each one is antiphase with all of its neighbors. Similar to how an optically controlled input is FALSE when it remains suppressed, we can consider an input in the steady state to be FALSE, because if it is perturbed and shifts out of the steady state, that perturbation will propagate to the output it is coupled to. However, when this new definition of an input is applied to a drop that is also the output of another gate, a contradiction becomes evident. When a drop is the input to a gate perturbing it shifts it from FALSE to TRUE, but when it is the output of a gate perturbing it shifts it from TRUE to FALSE! One can attempt to rectify this by switching the definitions of TRUE and FALSE for an input in the steady state, but then an output with two TRUE inputs in the steady state will remain unperturbed, so it will no longer have the same behavior as the NOR gate we have defined. For either definition, adding additional droplets between the output of one NOR gate and the input of another does not solve this problem.

How then can we connect multiple NOR gates? First let us consider an additional component to our system, which will incidentally increase its robustness. Instead of allowing droplets in the circuit that are not optically

controlled inputs to freely oscillate in the steady state, we can entrain them to periodic light pulses. If we use 2:1 entrainment, where there are two light pulses per spike of an entrained drop, we can define two discrete states: the state where the drop spikes after the first light pulse, and the state where the drop spikes after the second. Labeling one of these states to be TRUE and the other to be FALSE is more natural than constantly monitoring outputs to see whether they fall in a reading frame.

Since light pulses inhibit the droplets, if an entrained droplet is perturbed significantly enough, it will shift such that it spikes one light pulse later. This is preferable to our current system if you want to propagate a phase shift down a chain of drops. If a chain of drops begins in the steady state and the first one is perturbed, it will in turn delay the spike of the one next to it, which will delay its neighbor, and so on. There is no reason to believe that the resulting phase shift will be the same between each consecutive pair of drops. With light pulses it should be possible to entrain neighboring droplets such that if one is perturbed and switches states it will delay the next one enough to do the same.

Periodic illumination will also solve the problem of connecting multiple NOR gates. Let us revisit the case where the drops that make up a NOR gate begin in the steady state, and we define the inputs in this state to be TRUE. If we periodically illuminate the output for just under half a period, it will only be able to spike in the window where it is not suppressed. If we choose this window to such that the spikes of the inputs in the steady state occur at

its beginning, they will inhibit the output until it is illuminated again. If one input is perturbed and switches states, the other will still continue to inhibit the output. If both are perturbed, meaning they are now both FALSE, the output will no longer be inhibited in the window where it is not illuminated and can spike, propagating a TRUE signal to later in the circuit.

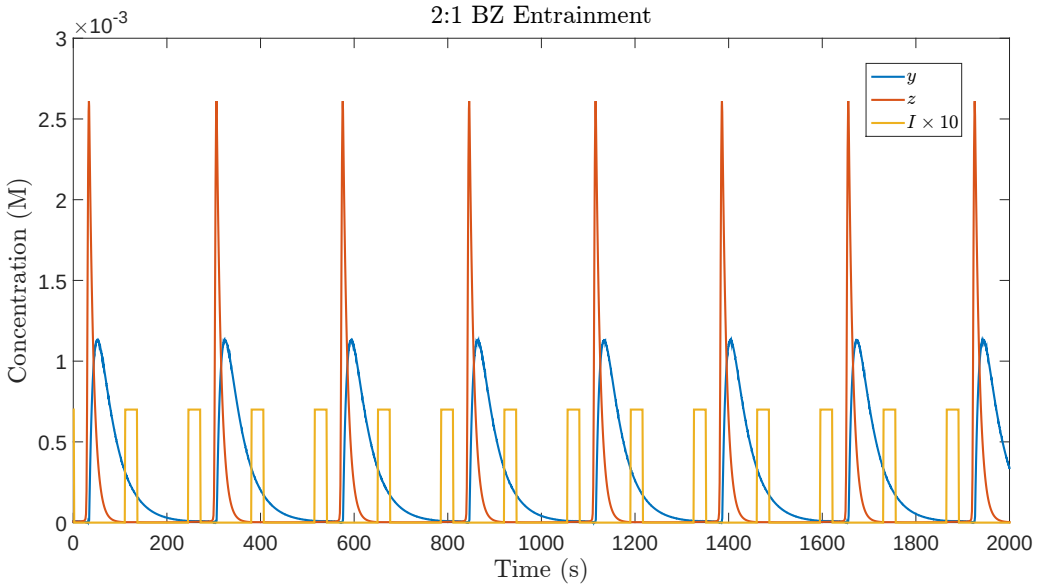

Figure 3.1: Plot of a BZ drop in 2:1 entrainment with light pulses. The plot was generated with the VE model in a preliminary investigation into entraining drops. Other simulations have demonstrated that under the right conditions it is possible to shift an entrained drop from one state to the other. We plan to conduct experiments to attempt to recreate both of these phenomena in a physical system.

Finally, one potential application of this research is in the fabrication of BZ robots. It has been shown that active chemomechanical hydrogels can be coupled to the BZ reaction [24, 25]. A network of BZ droplets used to perform computation could serve as a nervous system of sorts for such a gel,

where the droplets oscillate in such a way that the swelling and contracting of the gel produces locomotion.

Chapter 4

Bibliography

[1] Andrew Adamatzky, Ben De Lacy Costello, and Tomohiro Shirakawa. Universal computation with limited resources: Belousov-zhabotinsky and physarum computers. *International Journal of Bifurcation and Chaos*, 2008.

[2] Andrew Adamatzky, Benjamin De Lacy Costello, and Tetsuya Asai. *Reaction-Diffusion Computers*. Elsevier Science Inc., 2005.

[3] Boris P. Belousov. A periodic reaction and its mechanism. *Compilation of Abstracts on Radiation Medicine*, 1959.

[4] Benjamin De Lacy Costello and Andrew Adamatzky. Experimental implementation of collision-based gates in belousov-zhabotinsky medium. *Chaos, Solitons, and Fractals*, 2005.

[5] Jorge Delgado, Ning Li, Marcin Leda, Hector O. González-Ochoa, Seth Fraden, and Irving R. Epstein. Coupled oscillations in a 1d emulsion of belousov–zhabotinsky droplets. *Soft Matter*, 2011.

[6] Robert C Elson, Allen I Selverston, Ramon Huerta, Nikolai F Rulkov, Mikhail I Rabinovich, and Henry DI Abarbanel. Synchronous behavior of two coupled biological neurons. *Physical Review Letters*, 1998.

[7] C. Holtz et al. Biocompatible surfactants for water-in-fluorocarbon emulsions. *Lab on a Chip*, 2008.

[8] Hirokazu Fukuda, Hiroki Morimura, and Shoichi Kai. Global synchronization in two-dimensional lattices of discrete belousov–zhabotinsky oscillators. *Physica D: Nonlinear Phenomena*, 2005.

[9] Michael Heymann, Kyle I. Harrington, Jordan B. Pollack, and Seth Fraden. En route to signal inversion in chemical computing. In *ALIFE*, 2010.

[10] Julian Holley, Andrew Adamatzky, Larry Bull, Ben De Lacy Costello, and Ishrat Jahan. Computational modalities of belousov-zhabotinsky encapsulated vesicles. *Nano Communication Networks*, 2011.

[11] Eugene M. Izhikevich. *Dynamical Systems in Neuroscience: The Geomety of Excitability and Bursting*, chapter 10 (Synchronization). The MIT Press, 2007.

[12] Sandor Kadar, Takashi Amemiya, and Kenneth Showalter. Reaction mechanism for light sensitivity of the ru (bpy) 32+-catalyzed belousov-zhabotinsky reaction. *The Journal of Physical Chemistry A*, 1997.

[13] Ning Li, Nathan Tompkins, Hector Gonzalez-Ochoa, and Seth Fraden. Tunable diffusive lateral inhibition in chemical cells. *The European Physical Journal E*, 2015.

[14] Qinghua Liu, Liman Wang, Anthony G. Frutos, Anne E. Condon, Robert M. Corn, and Lloyd M. Smith. Dna computing on surfaces. *Nature*, 2000.

[15] Richard M. Noyes, Richard Field, and Endre Koros. Oscillations in chemical systems. i. detailed mechanism in a system showing temporal oscillations. *Journal of the American Chemical Society*, 1972.

[16] Mitsunori Ogihara and Animesh Ray. Simulating boolean circuits on a dna computer. *Algorithmica*, 1999.

[17] Manu Prakash and Neil Gershenfeld. Microfludic bubble logic. *Science*, 2007.

[18] Oliver Steinbock, Petteri Kettunen, and Kenneth Showalter. Chemical wave logic gates. *The Journal of Physical Chemistry*, 1996.

[19] Masahiro Toiya, Hector O. González-Ochoa, Vladimir K. Vanag, Seth Fraden, and Irving R. Epstein. Synchronization of chemical micro-oscillators. *The Journal of Physical Chemistry Letters*, 2010.

[20] Nathan Tompkins, Ning Li, Camille Girabawe, Michael Heymann, G. Bard Ermentrout, Irving R. Epstein, and Seth Fraden. Testing turings theory of morphogenesis in chemical cells. *Proceedings of the National Academy of Sciences*, 2014.

[21] Soichiro Tsuda, Masashi Aono, and Yukio-Pegio Gunji. Robust and emergent *Physarum* logical-computing. *Biosystems*, 2004.

[22] Alan Mathison Turing. On computable numbers, with an application to the entscheidungsproblem. *J. of Math*, 1936.

[23] Vladimir K. Vanag and Irving R. Epstein. A model for jumping and bubble waves in the belousov-zhabotinsky-aerosol ot system. *The Journal of Chemical Physics*, 2009.

[24] Ye Zhang, Ning Zhou, Sathish Akella, Yi Kuang, Dongshin Kim, Alyssa Schwartz, Marc Bezpalko, Bruce M. Foxman, Seth Fraden, Irving R. Epstein, et al. Active cross-linkers that lead to active gels. *Angewandte Chemie International Edition*, 2013.

[25] Ye Zhang, Ning Zhou, Ning Li, Megan Sun, Dongshin Kim, Seth Fraden, Irving R. Epstein, and Bing Xu. Giant volume change of active gels under continuous flow. *Journal of the American Chemical Society*, 2014.

Appendix A

Supplemental Information

A.1 FKN Mechanism

The following reactions make up the FKN mechanism which describes the BZ reaction:

$$\mathrm{BrO_3^-} + Br^- \xrightarrow{k_2} \mathrm{HOBr}$$

$$\mathrm{HBrO_2} + \mathrm{Br^-} + H^+ \xrightarrow{k_1} 2\mathrm{HOBr}$$

$$\mathrm{HOBr} + \mathrm{Br^-} + \mathrm{H^+} \underset{k_6}{\overset{k_5}{\rightleftharpoons}} \mathrm{Br_2} + \mathrm{H_2O}$$

$$\mathrm{Br_2} + \mathrm{CH_2(COOH)_2} \xrightarrow{k_7} \mathrm{BrCH(COOH)_2} + \mathrm{Br^-} + \mathrm{H^+}$$

$$\mathrm{BrO_3^-} + \mathrm{HBrO_2} + \mathrm{H^+} \underset{k_r}{\overset{k_4}{\rightleftharpoons}} 2\mathrm{BrO_2} + \mathrm{H_2O}$$

$$\mathrm{BrO_2} + \mathrm{Fe(phen)_3^{2+}} + \mathrm{H^+} \xrightarrow{k_{red}} \mathrm{HBrO_2} + \mathrm{Fe(phen)_3^{3+}}$$

$$2\mathrm{HBrO_2} \xrightarrow{k_3} \mathrm{BrO_3^-} + \mathrm{HOBr} + \mathrm{H^+}$$

$$\mathrm{HOBr} + \mathrm{CH_2(COOH)_2} \xrightarrow{k_8} \mathrm{BrCH(COOH)_2} + \mathrm{H_2O}$$

$$6\mathrm{Fe(phen)_3^{3+}} + \mathrm{CH_2(COOH)_2} + 2\mathrm{H_2O} \xrightarrow{k_{10}} 6\mathrm{Fe(phen)_3^{2+}} + \mathrm{HCOOH} + 2\mathrm{CO_2} + 6\mathrm{H^+}$$

$$4\mathrm{Fe(phen)_3^{3+}} + \mathrm{BrCH(COOH)_2} + 2\mathrm{H_2O} \xrightarrow{k_9} \mathrm{Br^-} + 4\mathrm{Fe(phen)_3^{2+}} + \mathrm{HCOOH} + 2\mathrm{CO_2} + 5\mathrm{H^+}$$

There are additional reactions which describe interactions with the photo-sensitive catalyst Rubpy:

$$\mathrm{Ru(bipy)_3^{2+}} + hv \xrightarrow{k_1} \mathrm{Ru(bipy)_3^{2+}}*$$

$$\mathrm{Ru(bipy)_3^{2+}}* + \mathrm{BrCH(COOH)_2} + \mathrm{H^+} \xrightarrow{k_C} \mathrm{Ru(bipy)_3^{3+}} + \mathrm{Br^-} + \text{products}$$

$$\mathrm{Ru(bipy)_3^{2+}}* \xrightarrow{k_d} \mathrm{Ru(bipy)_3^{2+}}$$

A.2 Simulation Parameters

Our simulations with the VE model use the following parameters:

$h = 0.15$	$a = 0.3$	$m = 0.6$	$c_0 = 0.003$
$k_1 = 2 \times 10^6 h$	$k_2 = 2h^2 a$	$k_3 = 3000$	$k_4 = 42ha$
$k_5 = 5 \times 10^9 h$	$k_6 = 10$	$k_7 = 29m$	$k_8 = 9.3m$
$k_r = 2 \times 10^8$	$k_{red} = 5 \times 10^6$	$k_9 = 0.12m$	$k_{10} = 0.05m$

$$c_{min} = \sqrt{\frac{2k_r(k_9 + k_{10})c_0}{k_{red}^2}}$$

$$b_c = 0.05$$

$$b = 0.1m$$

Acknowledgments

I would like to thank Professor Seth Fraden for advising me and giving me the opportunity to work on such an interesting project. I would not have achieved anywhere near this level of success without the collaboration of Adam Wang and all his hard work towards our final results. I am grateful to Kyle Harrington for inviting me to contribute to this project and sharing advice on what kinds of research to become involved in.

I would like to thank Professor Antonella DiLillo and Professor Hermann Wellenstein for giving me my first opportunities to work here at Brandeis. I would also like to thank Professor Irving Epstein and Professor Jordan Pollack for offering their time to be on my committee. I truly appreciate everything my professors, colleagues, friends, and family have done to support my current and future research.